Extraction and analysis of the characteristic parameters in back-to-back connected asymmetric Schottky diode

*Zuo Wang, Wanyu Zang, Yeming Shi, Xingyu Zhu, Gaofeng Rao, Yang Wang, Junwei Chu, Chuanhui Gong, Xiuying Gao, Hui Sun, Sibo Huanglong, Dingyu Yang and Peihua Wangyang**

Z. Wang, W. Zang, Y. Shi, X. Zhu, Dr. X. Gao, Dr. H. Sun, S. Huanglong, Prof. D. Yang, Dr. P. Wangyang
College of Optoelectronic Technology, Chengdu University of Information Technology, Chengdu, 610054, China.

G. Rao, Y. Wang, J. Chu, C. Gong, Dr. P. Wangyang
Electronic Thin Film and Integrated Devices, University of Electronic Science and Technology of China, Chengdu 610054, China
E-mail: wangyangpeihua@hotmail.com

Keywords: Schottky device, Thermionic emission theory, Barrier height, Ideality factor, Series resistance

Abstract: The physical Schottky parameters of the devices based on Schottky contact are important to analyze the working mechanism. This paper theoretically studies the parameter characteristics of current-voltage curve from two back-to-back connected Schottky contacts via the thermionic emission model, and it can be found that not all the parameters are able to be extracted under some constraints. Comparing with some classical extraction methods, a straightforward strategy to approach the Schottky intrinsic parameters by solving equations during characteristic interval are presented. Besides, this method is verified on several representative standard curves

This article has been accepted for publication and undergone full peer review but has not been through the copyediting, typesetting, pagination and proofreading process, which may lead to differences between this version and the Version of Record. Please cite this article as doi: 10.1002/pssa.201901018

and experimental curves, and the extracted parameters are highly compatible with those curves. The current extraction method would be of great significance for the design and preparation of Schottky based devices.

1. Introduction

Metal-semiconductor (MS) contacts are widely used in modern electronic devices.[1-7] Current MS contacts could be generally classified into: Ohmic contacts and Schottky contacts. In the ohmic contacts, there is no voltage drop through the MS interface which results in a symmetrical current-voltage curve obey Ohm's law. And in the Schottky contacts, there is a so-called space charge region on the semiconductor side, and potential barrier forms consequently.[1] This barrier causes rectifying behavior, and its diodes can be built into high frequency rectification, while reducing energy consumption and electronic noise, improving work efficiency and frequency.[8,9] In the applications, ideality factors, barrier heights and series resistance are important for designing and manufacturing the electronic devices.[5] Therefore, it is necessary to acquire the characteristic parameters of the Schottky diode. Fortunately, on the basis of thermionic emission theory, the current-voltage curve contains enough characteristics that can be effectively used in parameters extraction.[10-12]

There are many strategies put forward to extract parameters of MS diode impacted by a single Schottky barrier height.[13-29] In these articles, Bennett method is convenient and practical. All it needs is to select a certain range of forward bias to

solve a system of linear equations.[21] In recent years, nevertheless, parameters extraction techniques based on artificial intelligence using all kinds of algorithms have been developed, such as genetic algorithm, simulated annealing algorithm and differential evolution method, providing us a more accurate fitting scheme.[7,30-35] In addition, some methods for parameters extraction in back-to-back connected Schottky contacts were also developed in the last few years.[36-39] Nouchi found the identical region between MS contact and metal-semiconductor-metal (MSM) contact.[39] And in this identical region, an MSM diode can be regarded as an MS diode. Thus, there are only one group characteristics of single Schottky barrier parameters in the identical region. So, it is relatively simpler to extract those parameters of a single Schottky barrier first, and then extrapolate another Schottky barrier. But this method is inoperative when two barrier heights are too close to make the identical region invisible.

To the best of our knowledge, series resistance did not get enough attention in MSM contact. Moreover, there is still not enough research on the characteristic of all parameters in back-to-back connected Schottky contacts as well as the analysis of parameters validity. Based on thermionic emission theory, in this paper, the impact of ideal MSM contacts parameters on current-voltage curve in several certain conditions are analyzed. Besides, according to the characteristic interval, a method to approximate those parameters is proposed via solving equations. The results of our method are compared with those of Bennett method and we found it's highly

compatible with the experimental results. Our works provide a new and reliable solution for the parameter extraction of back-to-back connected Schottky contacts in the future.

2. Theory

When the Schottky barrier width is much smaller than the mean free path of electron, the current transfer through the interface is usually described by the thermionic emission.[40] The expression for the current is[41]

$$I = I_0[exp(\frac{\beta V}{n}) - 1] \quad (1)$$

with $\beta = \frac{q}{kT}$

$$I_0 = AA^{**}T^2\, exp(-\beta\phi_b) \quad (2)$$

and $A^{**} = \frac{4\pi q m^* k^2}{h^3}$

where I_0 is saturation current, β is the inverse thermal voltage, V is the potential drop, q is the unit electronic charge, k is the Boltzmann constant, T is the absolute temperature, A is the contact area, ϕ_b is the Schottky barrier height in volts , m^* is the effective mass of the charge carrier, h is the Planck constant, A^{**} is the effective Richardson constant, n is called the ideality factor. For thermionic emission, the ideality factor is equal to 1, and when other emission mechanisms such as field-enhanced tunneling and thermally assisted tunneling work on current transport, this parameter is larger than 1.[39]

Actually, as shown in **Figure 1**, the back-to-back connected asymmetric Schottky diodes are commonly employed in electronic device.[42] In this case, one

current flows through two back-to-back connected diodes with a series resistance and two voltage drops polarized in the opposite direction. According to **Equation 1**, voltage drop on the back-to-back connected Schottky diodes is sum of them on two interfaces and on series resistance[41]

$$V = V_1 + V_2 + RI = \frac{n_1}{\beta} ln(\frac{I}{I_{01}} + 1) - \frac{n_2}{\beta} ln(-\frac{I}{I_{02}} + 1) + RI \quad (3)$$

where R is the series resistance, V_1 and V_2 are the voltage drops on the forward and reverse polarized diodes, n_1 and n_2 are two different ideality factors of the two opposite diodes and I_{01} and I_{02} are two saturation currents of the two diodes, respectively.

3. General investigation of current-voltage curve

Standard representative current-voltage curves of back-to-back connected Schottky diodes with various combinations of parameters are generated from **Equation 3**, as shown in **Figure 2**. From Figure 2(a)-(d), one can see that I_{02} goes down as ϕ_2 increases. It is interesting to find that the ϕ_2 become indistinguishable thus making the current-voltage curves overlapped in a detectable coordinate scale as inset shown in Figure 2(a)-(d). However, indistinguishable curves of Figure 2(a)-(d) will eventually become recognizable when voltage is applied large enough in theory (the figure is not shown here). To figure out how the ideality factors and series resistance impact on Equation 3, four barrier heights conditions (1) $\phi_1 = 0.8V$, $\phi_2 = 0.75V$, (2) $\phi_1 = 0.4V$, $\phi_2 = 0.35V$, (3) $\phi_1 = 0.8V$, $\phi_2 = 0.4V$ and (4) $\phi_1 = 0.3V, 0.6V, 0.9V$, $\phi_2 = 0V$ are generalized. Those barrier heights are

combined with ideality factors (Figure 2(e)-(h)) and series resistance (Figure 2(i)-(l)), respectively. In Figure 2(e), two ideality factors n_1 and n_2 can be well distinguished from the curve of two large barriers. And it's worth noting that ideality factor n_1 is easier to distinguish than n_2. On the contrary, we can see that in two smaller barriers such as in Figure 2(f), neither ideality factors n_1 or n_2 can be distinguished, which makes the extraction of two ideality factors impossible. After that, in Figure 2(g), the barrier ϕ_1 is large and ϕ_2 is small. One can find that the ideality factors n_2 cannot be effectively identified which is similar to that in Figure 2(f). And n_1 in Figure 2(g) can be easily identified. Furthermore, in Figure 2(h), we fixed the barrier ϕ_2 to 0 and changed ϕ_1 and n_1 at the same time. It can be seen that the larger ϕ_1 is, the easier it is to distinguish n_1. According to Figure 2(e)-(h), the ideality factor of one Schottky diode become distinguishable only if the barrier height of this Schottky diode is big enough. Finally, the impact of series resistance R is also analyzed in Figure 2(i)-(l). In Figure 2(i), two barriers are so large that the resistance can only be distinguished by an order of magnitude greater than 1000000. In Figure 2(j), two barriers are small, which allows the resistance to be distinguished on the magnitude of several Ohms. Similarly, resistors in Figure 2(k) and 2(l) can also be distinguished by several Ohms. Therefore, according to Figure 2(i)-(l) the influence of series resistance can be seen on current-voltage curves only in the case when the series resistance is so high that it drives the current-voltage curves already in reverse direction of the studied diodes, either the first diode or the second one.

In general, the characteristics of parameters can be quickly understood by comparing the experimental current-voltage curve with Figure 2 during the practical analysis. In addition, based on the discussion above, some parameters can be effectively extracted from the experimental curve, while others cannot due to the barrier condition or actual voltage limitation.

Moreover, here we also propose two experiences to support the following parameter extraction scheme. It can be clearly seen in Figure 2(g) that the ideality factor n_1 determines the slope of linear part of curve under logarithmic coordinates, and Figure 2(k) implies that the series resistance R determines when the linear part bends down to form an exponential curve.

Furthermore, actual electronic devices are greatly affected by temperature, so the influences of temperature on the current-voltage curve are also analyzed. It can be seen from **Equation 2** that both temperature and Richardson constant can directly effect on saturation currents. And from Equation 3, temperature and saturation currents directly contribute to current-voltage curve. In order to simplify the effect of temperature on current-voltage curve during calculation, we suppose that effective Richardson constant stays the same as temperature varies over a certain range. A comparison of different temperatures at three different barriers conditions is shown in **Figure 3**. One can see that saturation currents in two directions go up as temperature increasing and the slope of linear part is gradually changed with temperature.

4. The proposed method

In order to understand Equation 3 better, it can be rewritten as

$$\frac{dV}{dI} = SR(I) + R$$

with $SR(I) = \frac{n_1}{\beta(I_{01}+I)} + \frac{n_2}{\beta(I_{02}-I)}$,

where function $SR(I)$ is named SR (Schottky related resistance, SR) function, which represents the resistance cause by two Schottky contact interfaces for the external resistance. **Figure 4** (a)-(d) shows SR function of different combinations of barrier heights with different ideality factors, the horizontal current ranges from I_{01} to I_{02}. One can see that n_1 and n_2 becomes discernible when current get close to I_{01} and I_{02}, as shown in Figure 4(a)-(d), respectively.

Figure 4(a) shows when the current approaches two saturated currents I_{01} and I_{02}, the SR tends to infinity, and the slope on current-voltage curve tends to zero (as shown in Figure 2 and Figure 3). Hence, theoretically the current corresponding to the curve slope of zero under positive and negative bias is the saturation current. In fact, the saturation current under reverse bias might be hidden by the image force and the tunneling effect.[40] It is reported that the measured current under bias of -0.1V is 96% of saturation current in the case for a nearly ideal single diode.[45] And usually it is difficult to determine the saturation current directly on the forward bias curve, but when I_{02} is much larger than I_{01} and n_1 is close to n_2, twice the maximum slope current is the most likely saturation current (See the extrapolate saturation current under forward bias of Supporting Information).

After obtaining saturation currents, the remaining parameters in the equation are ideality factors n_1, n_2 and series resistance R. In the view of these three parameters, the equation is simplified into a linear equation. Theoretically, the parameters n_1, n_2 and R can be solved by constructing a system of simultaneous equations of three points on current-voltage curve. However, in practical calculation, it might produce a great error by arbitrarily choosing three points to solve the equations. Hence, it is vital to find the characteristic interval of each parameter to reduce the error.

The Equation 3 can be rewritten as

$$V = \int_0^I \frac{dV}{dI} dI = \int_0^I \frac{n_1}{\beta(I_{01}+I)} dI + \int_0^I \frac{n_2}{\beta(I_{02}-I)} dI + \int_0^I R dI \quad (4)$$

Here the smaller saturation current named as I_{01} and the lager one named as I_{02}. According to the first part of **Equation 4** on the right side, when current is close to saturation current I_{01}, ideality factor n_1 will be distinctively amplified and this is the start point of the characteristic interval of n_1. As the current increases, the distinction of n_1 will not vanish but well accumulate till current infinitely approaches I_{02}. Hence, the region $[0.2I_{01},\ 0.9I_{02}]$ is chosen as the characteristic interval of n_1 in our calculation. And according to the second part of Equation 4 on the right side, n_2 is the same as n_1 and its characteristic interval becomes from $0.1I_{02}$ to $0.9I_{02}$. However, according to the third part of Equation 4 on the right side, the start point of characteristic interval of R only depends on the value of itself. If all saturation currents I_{01}, I_{02} and R are small, the start point of characteristic interval of R will not exist in a detectable interval as shown in Figure 2(i). In other words, R is

unapproachable. According to the discussion above, the selected characteristic intervals of ideality factors n_1 and n_2 in different barrier heights are shown in Figure 4(a)-(d), respectively.

In order to reduce the accidental errors caused by few points, three selected segments contained by the intersection of two characteristic intervals are used to solve the equations (see Figure 4(e)). As shown in Figure 4e, the current intervals I_f, I_m and I_n with corresponding voltage intervals V_f, V_m and V_n form three divided sections. The system of simultaneous equations (named System 1st) expressed as

$$V_f = \frac{n_1}{\beta} ln(\frac{I_f}{I_{01}} + 1) - \frac{n_2}{\beta} ln(-\frac{I_f}{I_{02}} + 1) + RI_f \quad (5a)$$

$$V_m = \frac{n_1}{\beta} ln(\frac{I_m}{I_{01}} + 1) - \frac{n_2}{\beta} ln(-\frac{I_m}{I_{02}} + 1) + RI_m \quad (5b)$$

$$V_n = \frac{n_1}{\beta} ln(\frac{I_n}{I_{01}} + 1) - \frac{n_2}{\beta} ln(-\frac{I_n}{I_{02}} + 1) + RI_n \quad (5c)$$

where I_f, I_m, I_n, V_f, V_m and V_n are the data from each interval. After cross matching every data in the interval to establish simultaneous equations, there are $f \times m \times n$ simultaneous equations. After obtaining parameter result groups, the frequency diagrams of those parameter groups are drawn to select the appropriate parameters. If the selected points distributed evenly in the SR function, the results should be accord with Gaussian distribution in theory. And expected value of the distribution is consequently chosen as the value of the parameter. But in practice, there might be one or several influence factors contributing a lot to the value of parameters, makes the results do not fit Gaussian distribution. So, to fix this deviation, we need to select the mode of results as the value of parameters. If the curve is not

complete enough to find out ideality factor n_2 or series resistance R which will result in an unreasonable frequency diagram, fix n_2 as unity to solve the equations system (named System 2nd) with two unknowns. Without ideality factor n_2, the adopted data is from two segments which is divided on average from the characteristic interval of n_1.

To verify the reliability of calculated parameters, the final step is to draw the curve with the calculated parameters, compare it with the experimental curve, and then fine-tune them according to the rules summarized above. And the general flowchart of our strategy to approach the parameters is detailed in **Figure 5**.

5. Results and discussion

To verify the accuracy of the method above and as a demonstration, this method is used on several representative curves generated according to Equation 3 at room temperature. Following the flowchart (Figure 5), we first manually take points from the generated standard curve, as shown in part (a) of Figure S1-S6. After that, the saturation currents are obtained from the end point of the picked curves, and SR function (image (b) of Figure S1-S6) was drawn to select the characteristic interval. And after the calculation by substituting data into Equation (5a), (5b) and (5c), the frequency diagram of two ideality factors and series resistance are drawn (see Figure S1-S6). One can see that the diagrams of Figure S1, Figure S2, Figure S5 and Figure S6 are reasonable, and the parameter values are adopted to fitting curves (image (f) of Figure S1, Figure S2, Figure S5 and Figure S6). However, in Figure S6(e), the series

resistance R is not large enough to be identified comparing with Figure S5(e). Besides, in Figure S3(d), the barrier heights are too small to identify the ideality factor n_2 from generated curve. Hence, we fix n_2 as 1 to resolve the System 2nd (as shown in Figure S3(f), S3(g), S4(c) and S4(d)). Furthermore, the value of n_2 is varied to show its validity in Figure S4(f), from which one can see n_2 is indistinguishable within a reasonable range of values. In other words, we can assume that n_2 is any value in the range much smaller than 10^5 and this does not affect the solution, meanwhile, n_2 itself have lost physical meaning and become a technical parameter. For simplicity, n_2 can always be set as 1. What need to be state here is that ideality factor n_2 in Figure S4 and Figure S6 is too large to be described completly by thermionic emission, that means n_2 in these figures are also just technical parameters. But from n_2 in Figure S4 one can see that n_2 cannot be extracted even if n_2 is large as 5, and in Figure S5 and Figure S6 one can see that n_2 is accessable no matter n_2 it self is small or large when barrier of this diode allows it. As a result, all simulations are in **Figure 6**, and the parameters extracted are compared with standard parameters in **Table 1**. More details are shown in Supporting Information (Figure S1-S6). By comparing Figure 6 and Table 1, it can be seen that the parameters obtained by our method is very consistent with the original parameters, which indirectly proves that this is an effective extraction method.

Moreover, in order to further verify the feasibility of our method, four reported current-voltage curves from previous articles are chosen for the extraction process as

the result shown in **Figure 7** with **Table 2-6**.[43-46] In those fitting curves, literature fitting only presented us one ideality factor or with one barrier height (see Table 2 and 6), while rest of parameters that Equation 3 needed are from our result. Besides, curves fitted by Bennett method in Figure 7 all use the single diode model which conform Equation 1. And the adopted interval for Bennett's calculation is the identical region found by Nouchi.[21,39] Therefore, the green curves always go up exponentially under a large forward bias. As a part of extraction procedure, our fitting parameters before fine-tune are also shown in Table 2, 3 and 6. Furthermore, the unsaturated current under reverse bias in Figure 7(c) was fitted using least square method by thermionic-field emission mechanism under reverse bias (see Figure S9). In those extracted parameters, the barrier heights in Figure 7(a) can be obtained from Equation 2 theoretically (not given here due to the lack of area A in Equation 2) and the barrier heights in other figures were calculated using the standard Richardson constant ($A^{**} = 1.2 \times 10^6 Am^{-2}K^{-2}$) (given experimental data is current density-voltage, hence, the area A in Equation 2 is unnecessery to come out barrier height). It can be extrapolated that barrier ϕ_2 in Table 2 and 3 are both not large enough to make n_2 distinguishable, hence it is more reasonable to fix n_2 as unity. However, in the case of Table 6 the characteristic intervals of n_2 and R are overlapped and the result becomes doubtable, because the fitting curve of $n_2 = 1$ and $RA = 1.5\Omega m^2$ are almost overlapped with the curve of $n_2 = 1.5$ and $RA = 0\Omega m^2$ (see Figure S10(p)). From Figure 7 and Table 2-5, One can see the

fitting curves are highly compatible with experimental curves, it indicates our extraction method is effective. More details are shown in Supporting Information (Figure S7-S10).

6. Conclusions

In summary, the current-voltage characteristics of MSM diodes under varies impacts of parameters were investigated. From the investigation of characteristic parameters of two back-to-back connected Schottky contacts, we present two empirical conclusions: (a) Ideality factor of one Schottky diode become distinguishable in the detectable coordinate scale only if the barrier height of this Schottky diode is high enough. (b) Series resistance is recognized only when the series resistance is big enough that it drives the current-voltage curves already in reverse direction of the studied diodes, either the first diode or the second one.

A method via solving equations during characteristic interval was proposed to extract the parameters from the current-voltage curve of two back-to-back connected Schottky contacts. The Schottky parameters of MSM interface could be calculated by the following procedure: (a) Saturation currents must be attainable or conjecturable from the current-voltage curve and barrier heights can be derived. If two saturation currents are hidden by an incomplete curve or others physical mechanism, try to treat the measured current under bias of -0.1V as reverse saturation current, and the extrapolation of forward saturation current can be seen in Supporting Information. (b) Plot the SR function to select appropriate intervals of current and voltage. (c) Solve

System 1st established by cross matching each point in the intervals of current and voltage. (d) Choose values from the frequency diagrams of parameters. If the frequency diagrams are not adoptable, reselect the intervals to calculate System 2nd. (e) Draw the curve using calculated results and compare with original curve. If there is any deviation, fine-tune the curve according to the following experiences: Ideality factor n_1 determines the slope of linear part of curve under logarithmic coordinates, and series resistance R determines when the linear part bends down to form an exponential curve. Comparing standard curves with our simulations, it can be seen that this method is highly feasible. Moreover, this method is verified through the extraction of experimental curves, and the curves from extracted parameters are compatible with the experimental curves.

Supporting Information

The Supporting Information is available free of charge. Extrapolate saturation current under forward bias, extraction process on standard curves and experimental curves.

Acknowledgements

This work was partially supported by the China Postdoctoral Science Foundation (Grant No. 2018M643443), National Natural Science Foundation of China (Grant No. 51802032 and 11675029), Science and Technology Research Fund of Sichuan Province (Grant No. 2017JY0320 and 2018JY0513), and National undergraduate innovation and entrepreneurship training program (Grant No. 201810621051 and S201910621092).

Conflict of Interest

The authors declare no conflict of interest.

Received: ((will be filled in by the editorial staff))
Revised: ((will be filled in by the editorial staff))
Published online: ((will be filled in by the editorial staff))

References :

[1]W. Tian, H. Sun, L. Chen, P. Wangyang, X. Chen, J. Xiong, L. Li, *InfoMat.* **2019**, *1*, 140-163.

[2]C. Yan, C. Gong, P. Wangyang, J. Chu, K. Hu, C. Li, X. Wang, X. Du, T. Zhai, Y. Li, J. Xiong, *Adv. Funct. Mater.* **2018**, *28*, 1803305.

[3]C. Gong, K. Hu, X. Wang, P. Wangyang, C. Yan, J. Chu, M. Liao, L. Dai, T. Zhai, C. Wang, L. Li, J. Xiong, *Adv. Funct. Mater.* **2018**, *28*, 1706559.

[4]J. Chu, F. Wang, L. Yin, L. Lei, C. Yan, F. Wang, Y. Wen, Z. Wang, C. Jiang, L. Feng, J. Xiong, Y.Li, J. He, *Adv. Funct. Mater.* **2017**, *27*, 1701342.

[5]J. Wang, J. Han, X. Chen, X. Wang, *InfoMat.* **2019**, *1*, 33-53.

[6]G. Rao, X. Wang, Y. Wang, P. Wangyang, C. Yan, J. Chu, L. Xue, C. Gong, J. Huang, J. Xiong, Y. Li, *InfoMat*. **2019**, *1*, 272-288.

[7]A. Sellai, Z. Ouennoughi, *Int. J. Mod. Phys. C* **2005**, *16*, 1043-1050.

[8]E. H. Rhoderick, E. Rhoderick, *Metal-Semiconductor Contacts*, Clarendon Press, Oxford **1978**.

[9]S. M. Sze, K. K. Ng, *Physics of Semiconductor Devices*, Wiley, Hoboken, NJ **2006**.

[10]K. Akkiliç, M. E. Aydin, A. Türüt, *Phys. Scr.* **2004**, *70*, 364.

[11]M. E. Aydin, K. Akkiliç, T. Kiliçoğlu, *Appl. Surf. Sci.* **2006**, *253*, 1304-1309.

[12]G. Liang, T. Cui, K. Varahramyan, *Solid-State Electron.* **2003**, *47*, 691-694.

[13] H. Norde, *J. Appl. Phys.* **1979**, *50*, 5052-5053.

[14] K. Sato, Y. Yasumura, *J. Appl. Phys.* **1985**, *58*, 3655-3657.

[15] C. D. Lien, F. C. T. So, M. A. Nicolet, *IEEE Trans. Electron Devices* **1984**, *31*, 1502-1503.

[16] S. K. Cheung, N. W. Cheung, *Appl. Phys. Lett.* **1986**, *49*, 85-87.

[17] J. H. Werner, *Appl. Phys. A* **1988**, *47*, 291-300.

[18] D. Donoval, M. Barus, M. Zdimal, *Solid-State Electron.* **1991**, *34*, 1365-1373.

[19] V. Aubry, F. Meyer, *J. Appl. Phys.* **1994**, *76*, 7973-7984.

[20] J. Osvald, E. Dobročka, *Semicond. Sci. Technol.* **1996**, *11*, 1198-1202.

[21] R. J. Bennett, *IEEE Trans. Electron Devices* **1987**, *34*, 935-937.

[22] V. Mikhelashvili, G. Eisenstein, R. Uzdin, *Solid-State Electron.* **2001**, *45*, 143-148.

[23] A. Ferhat-Hamida, Z. Ouennoughi, A. Hoffmann, R. Weiss, *Solid-State Electron.* **2002**, *46*, 615-619.

[24] D. Gromov, V. Pugachevich, *Appl. Phys. A* **1994**, *59*, 331-333.

[25] R. M. Cibils, R. H. Buitrago, *J. Appl. Phys.* **1985**, *58*, 1075-1077.

[26] K. E. Bohlin, *J. Appl. Phys.* **1986**, *60*, 1223-1224.

[27] A. Ortiz-Conde, Y. Ma, J. Thomson, E. Santos, J. J. Liou, F. J. G. Sánchez, M. Lei, J. Finol, P. Layman, *Solid-State Electron.* **1999**, *43*, 845-848.

[28] E. K. Evangelou, L. Papadimitriou, C. A. Dimitriades, G. E. Giakoumakis, *Solid-State Electron.* **1993**, *36*, 1633-1635.

[29] A. Ortiz-Conde, F. J. G. Sanchez, *Solid-State Electron.* **2005**, *49*, 465-472.

[30] A. Sellami, M. Zagrouba, M. Bouaïcha, B. Bessaïs, *Meas. Sci. Technol.* **2007**, *18*, 1472-1476.

[31] Y. Li, *Microelectron. Eng.* **2007**, *84*, 260-272.

[32] F. Li, S. P. Mudanai, Y.-Y. Fan, W. Zhao, L. F. Register, S. K. Banerjee, in *Proc. 15th Biennial University/Government/Industry Microelectronics Symposium (Cat. No. 03CH37488)*, Boise, USA, July **2003**.

[33] M. Thomas, C. Pacha, K. Goser, in *Proc. International Conference on Computational Intelligence*, Dortmund, Germany, May **1999**.

[34] K. Wang, M. Ye, *Solid-State Electron.* **2009**, *53*, 234-240.

[35] B. Lakehal, A. Dendouga, *J. Nano- Electron. Phys.* **2018**, *10*, 06046-1-06046-4.

[36] A. J. Chiquito, C. A. Amorim, O. M. Berengue, L. S. Araujo, E. P. Bernardo, E. R. Leite, *J. Phys.: Condens Matter* **2012**, *24*, 225303.

[37] M. Ahmetoglu, S. K. Akay, *Curr. Appl. Phys.* **2010**, *10*, 652-654.

[38] V. Mikhelashvili, R. Padmanabhan, G. Eisenstein, *J. Appl. Phys.* **2017**, *122*, 034503.

[39] R. Nouchi, *J. Appl. Phys.* **2014**, *116*, 184505.

[40] E. H. Rhoderick, R. H. Williams, *Metal-Semiconductor Contacts*, 2nd Edn. Clarendon Press, Oxford, **1988**.

[41] J. Osvald, *Phys. Status Solidi A* **2015**, *212*, 2754-2758.

[42] F. Hernandez-Ramirez, A. Tarancon, O. Casals, E. Pellicer, J. Rodriguez, A. Romano-Rodriguez, J. R. Morante, S. Barth, S. Mathur, *Phys. Rev. B* **2007**, *76*, 085429.

[43] F. Guo, B. Yang, Y. Yuan, Z. Xiao, Q. Dong, Y. Bi, J. Huang, *Nat. Nanotechnol.* **2012**, *7*, 798.

[44] G. Li, Z. Li, J. Chen, X. Chen, S. Qiao, S. Wang, Y. Xu, Y. Mai, *J. Alloys Compd.* **2018**, *737*, 67-73.

[45] Y. Liu, J. Guo, E. Zhu, L. Liao, S. J. Lee, M. Ding, I. Shakir, V. Gambin, Y. Huang, X. Duan, *Nat.* **2018**, *557*, 696-700.

[46] B. C. Min, K. Motohashi, C. Lodder, R. Jansen, *Nat. Mater.* **2006**, *5*, 817-22.

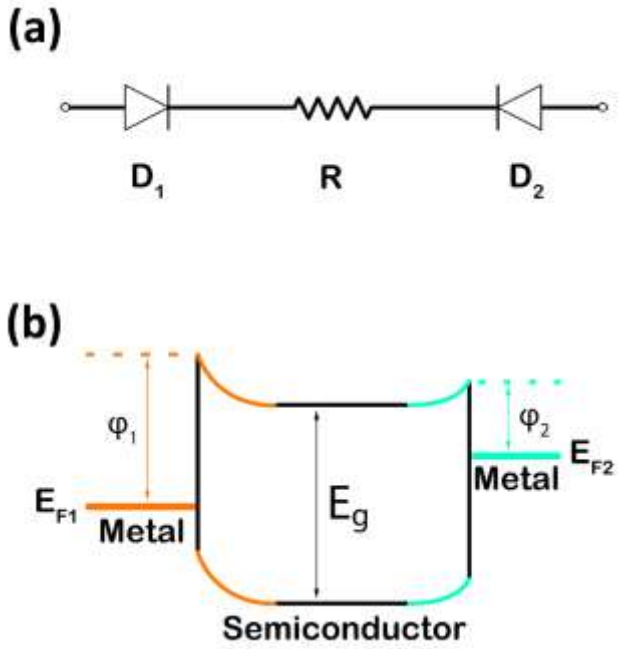

Figure 1. a) Two Schottky barriers connected back-to-back with series resistance. (b) The energy band diagram of MSM contact with different barrier heights and n-type semiconductor under equilibrium, besides, external bias is applied.

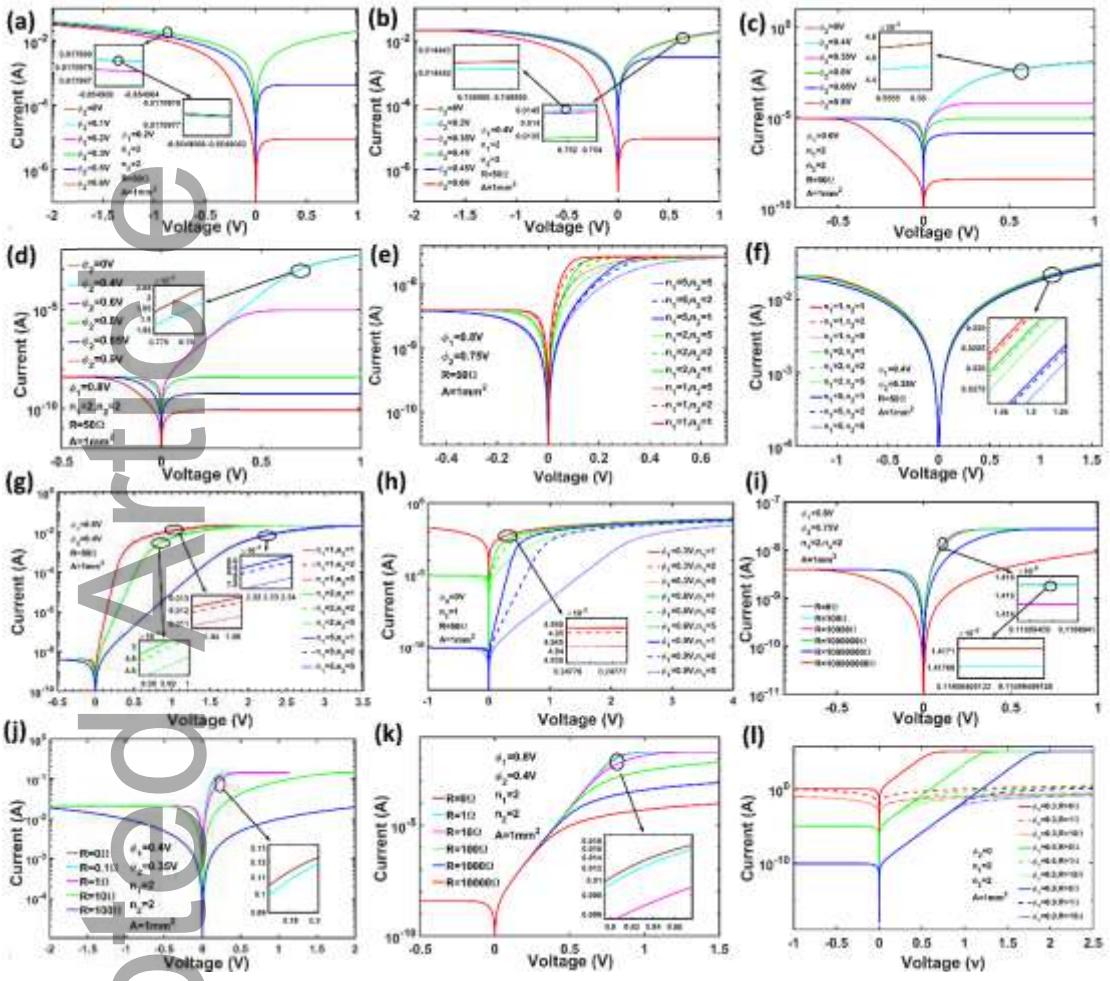

Figure 2. Current-voltage curves of back-to-back asymmetric Schottky diodes in various conditions of barrier heights, ideality factors and series resistance. The barrier height ϕ_2 varied and ϕ_1 is fixed as (a) 0.2V, (b) 0.4V, (c) 0.6V and (d) 0.8V, respectively. Various combinations of ideality factors with (e) $\phi_1 = 0.8V$, $\phi_2 = 0.75V$, (f) $\phi_1 = 0.4V$, $\phi_2 = 0.35V$, (g) $\phi_1 = 0.8V$, $\phi_2 = 0.4V$. Various ideality factor n_1 and ϕ_1 with fixed $\phi_2 = 0V$ (h). Various series resistance R with (i) $\phi_1 = 0.8V$, $\phi_2 = 0.75V$, (j) $\phi_1 = 0.4V$, $\phi_2 = 0.35V$, (k) $\phi_1 = 0.8V$, $\phi_2 = 0.4V$. Various series resistance R and ϕ_1 with fixed $\phi_2 = 0V$ (l).

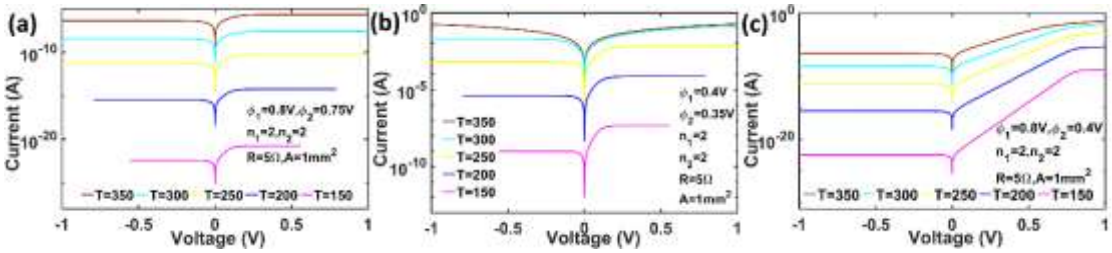

Figure 3. Current-voltage curve changes with several temperatures in three different barrier conditions: (a) $\phi_1 = 0.8V,\ \phi_2 = 0.75V$, (b) $\phi_1 = 0.4V,\ \phi_2 = 0.35V$ and (c) $\phi_1 = 0.8V,\ \phi_2 = 0.4V$, respectively.

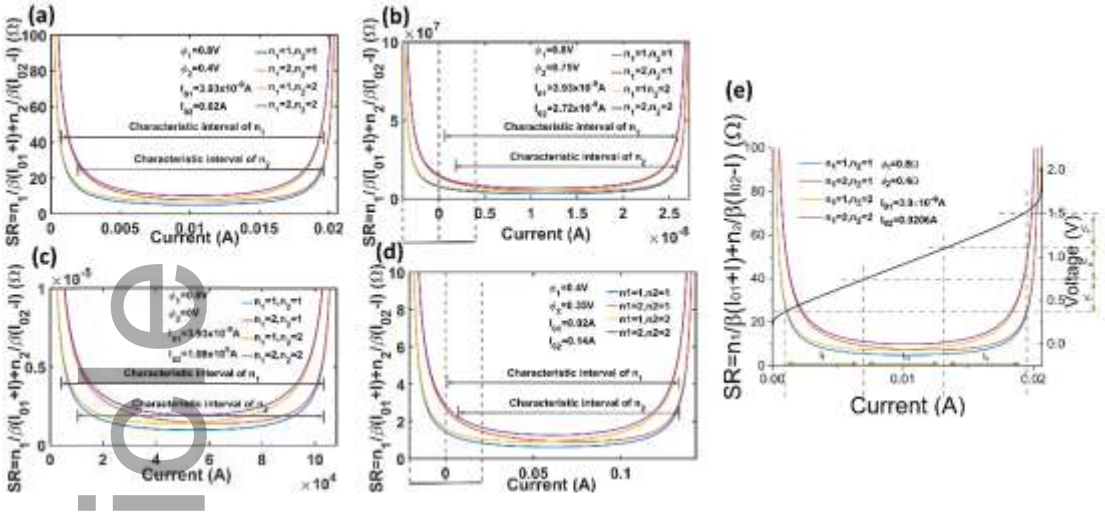

Figure 4. SR function under barrier heights of (a) $\phi_1 = 0.8V$, $\phi_2 = 0.4V$, (b) $\phi_1 = 0.8V$, $\phi_2 = 0.75V$, (c) $\phi_1 = 0.8V$, $\phi_2 = 0V$ and (d) $\phi_1 = 0.4V$, $\phi_2 = 0.35V$. (e) Schematic diagram of interval selection for current and voltage under $\phi_1 = 0.8V$, $\phi_2 = 0.4V$.

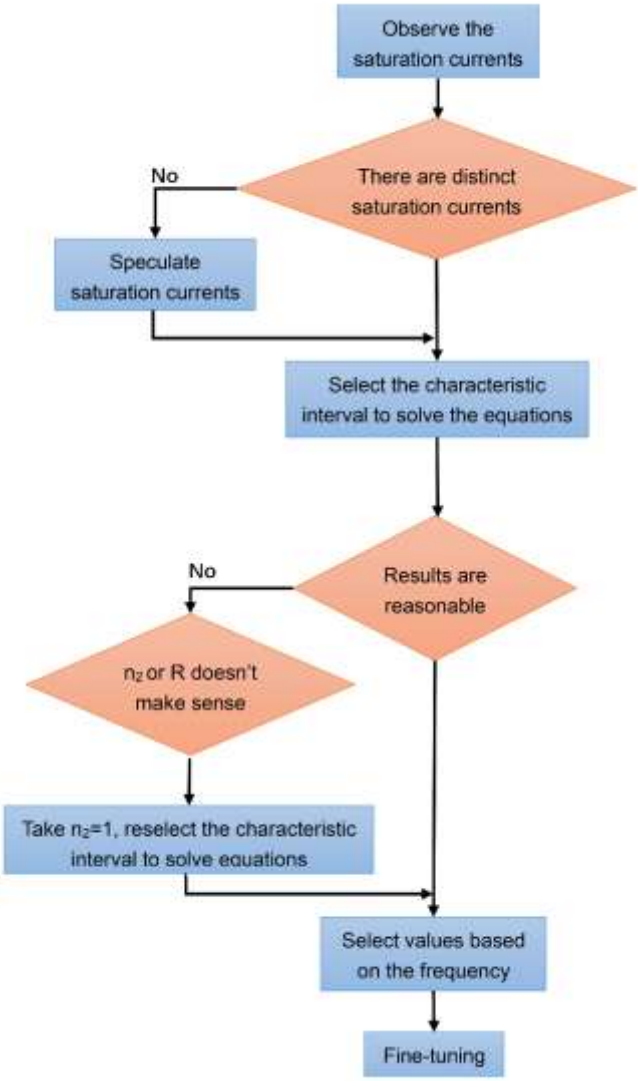

Figure 5. The flowchart of our extraction strategy.

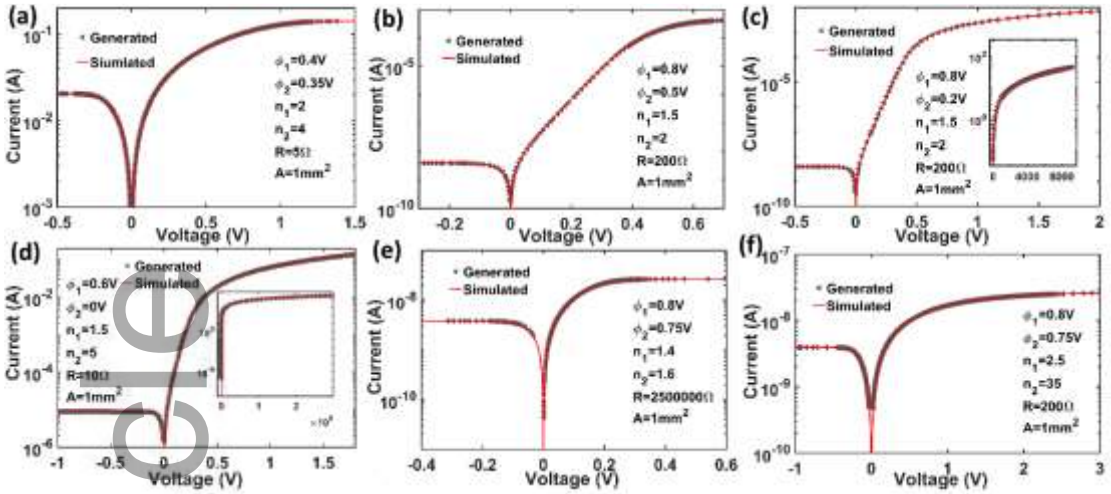

Figure 6. Standard curves generated comparing with our fitting curves. (a) In both barrier heights are low and the difference is small ($\phi_1 = 0.4V$ and $\phi_2 = 0.35V$). (b) and (c) The same series resistances (R = 200Ω) in two different barrier heights. (d) The extreme condition when $\phi_1 = 0.6V$ and $\phi_2 = 0V$. (e) and (f) The same barrier heights ($\phi_1 = 0.8V$ and $\phi_2 = 0.75V$) in two different series resistances.

Table 1 Standard parameters and extracted parameters in Figure 6.

	Figure 6 (a)		Figure 6 (b)		Figure 6 (c)		Figure 6 (d)		Figure 6 (e)		Figure 6 (f)	
	Generated	Our result	Generated	Our result	Generated	Our result	Generated	Our result	Generated	Our result	Generated	Our result
ϕ_1 (V)	0.4	0.4001	0.8	0.8001	0.8	0.8001	0.6	0.6004	0.8	0.8006	0.8	0.8
ϕ_2 (V)	0.35	0.3501	0.5	0.5001	0.2	0.2001	0	0.0013	0.75	0.7503	0.75	0.7501
n_1	2	2	1.5	1.497	1.5	1.49	1.5	1.52	1.4	1.52	2.5	2.6
n_2	4	4	2	1.87	2	-	5	-	1.6	1.7	35	35
$R(\Omega)$	5	5	200	210	200	201	10	10	2500000	2200000	200	-

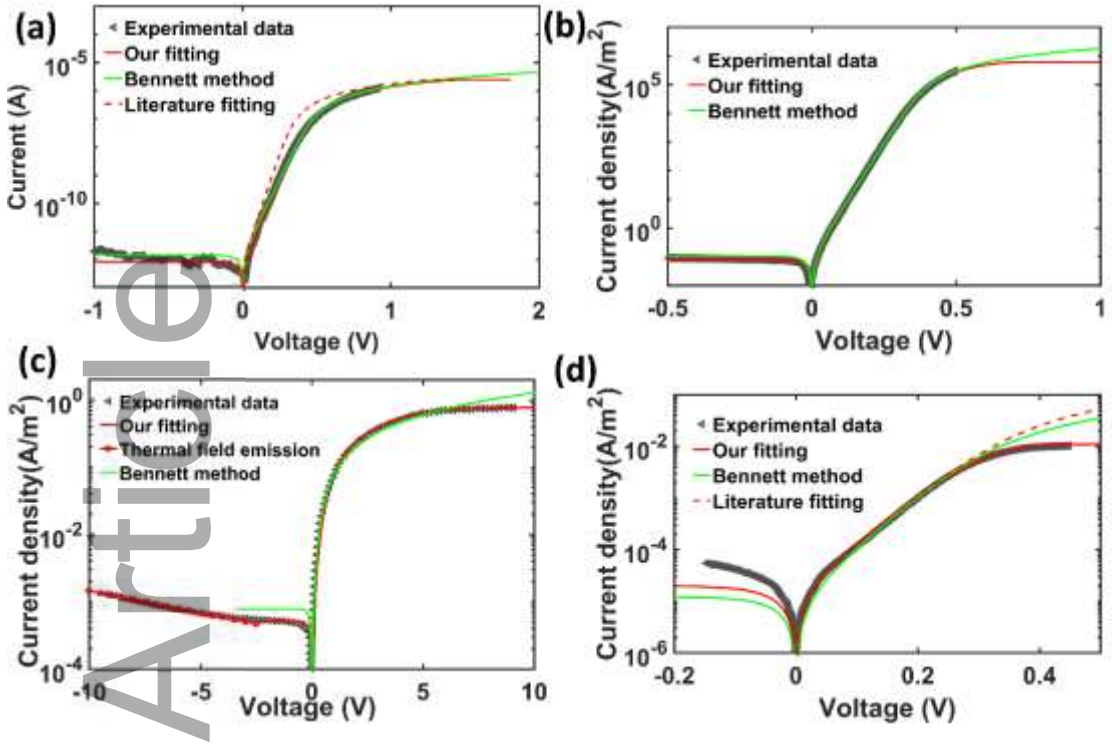

Figure 7. Previously reported experimental curves with several simulations. (a) Experimental curve comparing with our fitting, Bennett fitting and literature fitting. (b) Experimental curve with our fitting and Bennett method. (c) Experimental curve with our fitting, Bennett method and thermal field emission fitting. (d) Experimental curve with our fitting, Bennett fitting and literature fitting.

Table 2 Parameters of all curves in Figure 7(a).

	I_{01}(A)	I_{02}(A)	n_1	n_2	$R(\Omega)$
Literature fitting	-	-	1.09	-	-
Our fitting before fine-tune	6.5×10^{-13}	2.51×10^{-6}	1.36	1	3.2×10^{5}
Our fitting	8×10^{-13}	2.51×10^{-6}	1.45	1	3.2×10^{5}
Bennett method	1.43×10^{-12}	-	1.55	-	3.04×10^{5}

Table 3 Parameters of all curves in Figure 7(b).

	ϕ_1 (V)	ϕ_2 (V)	n_1	n_2	$RA(\Omega m^2)$
Our fitting before fine-tune	0.7240	0.3122	1.01	1	3.5×10^{-7}
Our fitting	0.7196	0.3122	1.04	1	3×10^{-7}
Bennett method	0.7148	-	1.33	-	1.2×10^{-6}

Table 4 Parameters of all curves in Figure 7(c).

	ϕ_1 (V)	ϕ_2 (V)	n_1	n_2	$RA(\Omega m^2)$
Our fitting	0.8523	0.6635	4.43	34	4
Bennett method	0.8418	-	3.67	-	7.25

Table 5 Reverse bias fitting in Figure 7(c).

$\lvert J\rvert = ae^{bV}(c+V)^{(1/2)}$	a	b	c
Reverse bias fitting	3.18×10^{-6}	-0.15	1×10^{4}

Table 6 Parameters of all curves in Figure 7(d).

	ϕ_1 (V)	ϕ_2 (V)	n_1	n_2	$RA(\Omega m^2)$
Literature fitting	0.9044	-	1.9	-	-
Our fitting before fine-tune	0.9365	0.7734	1.97	1	1.5
Our fitting	0.9365	0.7734	1.9	1	1.5
Bennett method	0.9493	-	1.33	-	4.16

Keyword
Schottky device, Thermionic emission theory, Barrier height, Ideality factor, Series resistance

*Zuo Wang, Wanyu Zang, Yeming Shi, Xingyu Zhu, Gaofeng Rao, Yang Wang, Junwei Chu, Chuanhui Gong, Xiuying Gao, Hui Sun, Sibo Huanglong, Dingyu Yang and Peihua Wangyang **

Extraction and analysis of the characteristic parameters in back-to-back connected asymmetric Schottky diode

ToC figure

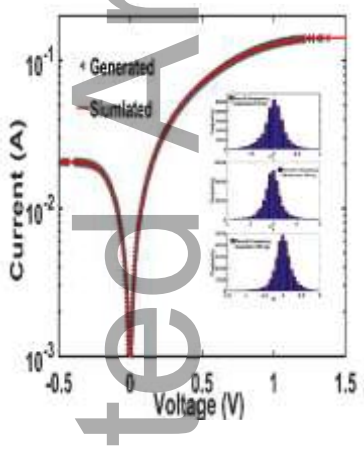

The characteristic parameters of the Schottky diode appear essential to evaluate the properties of electronic devices. This paper emphasizes not all parameters are able to be extracted under some constraints. A straightforward strategy to approach the Schottky intrinsic parameters by solving equations during characteristic interval is presented and verified. The extraction method would be of great significance for electron device.